14TH CANADIAN MASONRY SYMPOSIUM
MONTREAL, CANADA
MAY 16TH – MAY 20TH, 2021

NUMERICAL STUDY OF THE RESPONSE OF REINFORCED SLENDER MASONRY WALLS WITH VARIOUS REINFORCEMENT ARRANGEMENTS

Gonzalez, Rafael[1]; Alonso, Alan[2]; Cruz, Carlos[3] and Tomlinson, Douglas[4]

ABSTRACT

Single-storey Slender Masonry Walls (SMW) with low axial loads are commonly built in Canada. Provisions in the Canadian masonry standard CSA S304-14 require walls with a slenderness ratio of 30, or greater, to satisfy several stringent requirements. The reason for these restrictions is that slender walls are susceptible to second-order (P-Delta) effects and instability issues. Some simple solutions exist to reduce this problem, such as increasing steel reinforcement ratios and increasing the rebar depth relative to the compressive face of the wall section. These changes result in stiffer walls which reduce second-order effects, without the use of thicker and heavier CMUs (Concrete Masonry Units). However, recommendations on clear spacing and ductility behaviour provided in Canadian standards prevent, to some extent, the use of these solutions. With the use of an OpenSEES computer model, this study presents a parametric analysis of SMWs to understand their response when changing parameters such as the reinforcement arrangement and the materials strength. The results showed that increasing reinforcement ratio and rebar depth is the most efficient way to stiffen these walls. Three groups of walls with different steel reinforcement ratios ranging from under- to over-reinforced were analyzed. Each group consists of four sections with different steel reinforcement depth. From all these analyses, the authors present a promising solution to the previously mentioned issues, and propose further discussion to determine if code provisions are overly conservative and prevent engineers from designing more efficient configurations.

KEYWORDS: *analytical simulation, finite element, masonry walls, out of plane, slender walls*

[1] MSc Student, University of Alberta, 9211-116th St., Edmonton, AB, Canada, rafaelde@ualberta.ca
[2] PhD Student, University of Alberta, 9211-116th St., Edmonton, AB, Canada, alonsori@ualberta.ca
[3] Associate Professor, University of Alberta, 9211-116th St., Edmonton, AB, Canada, cruznogu@ualberta.ca
[4] Assistant Professor, University of Alberta, 9211-116th St., Edmonton, AB, Canada, dtomlins@ualberta.ca

INTRODUCTION

Slender masonry walls are widely used in single-storey buildings, such as gymnasiums and light industrial structures. These walls are susceptible to second-order effects and instability because of their limited flexural stiffness and their tendency to buckle under relatively low axial compression loads. For these reasons, they are restricted by special requirements in the Canadian masonry design standard CSA S304-14 [2]. In conventional Reinforced Masonry (RM) construction, steel reinforcement is placed at the centre of the wall. This practice results in inefficient use of reinforcement because it is close to the out-of-plane neutral axis (NA). To overcome this issue, various solutions have emerged for placing the reinforcement farther from the NA.

Near-surface Mounted (NSM) reinforcement is a technique where reinforcement is adhered to the tension side of a structural element to increase strength and stiffness. NSM reinforcement has been extensively used to retrofit structures, cutting groves into walls and placing the reinforcement with epoxy or a cementitious material [3, 4]. Sparling et al. [5] introduced a new Surface Reinforced (SR) CMU with a pair of channels on the external faces to include NSM reinforcement during the construction of new walls. Enough units were fabricated to build a series of 3.2 m tall by 1.2 m wide panels. Results showed that RM walls with NSM reinforcement using the same steel ratio have higher strength and stiffness than those with a conventional configuration. However, this wall system may come with challenges related to installation times and structural fire-safety.

Entz [6] improved the reinforcement scheme inside the blocks with pre-tied steel cages with specially designed CMUs that are able to slide around the cage to form an in-line boundary element, similar to an embedded concrete column. In this system, the increase in the moment arm of the reinforcement played a major role in reducing Out of Plane (OOP) deflections in loadbearing RM walls. This system enhanced the pre-cracked response, but after cracking the flexural stiffness of the enhanced wall and the conventional wall started to converge. The primary mechanism by which the OOP stiffness is enhanced is through inducing a compressive force in the rebar layer placed in the compression zone. Therefore, this is better suited for high axial load conditions.

In this study, a finite element model was developed using the OpenSEES software framework [1] to perform a parametric analysis in order to understand the overall behaviour of slender walls under different configurations, and then to analyse and compare an innovative arrangement with other more traditional options. This new configuration of 20 cm thick Partially Grouted (PG) RM walls was proposed placing the steel rebar touching the unit face shell to take advantage of a higher moment arm to resist moments and potentially achieve stiffer SMWs. This solution may present challenges during physical tests, such as a reduced bonding of the rebar to the concrete or early damage to the block face shell; however, the focus of this study was on the potential enhancements that can be achieved. Physical tests of full-scale SMWs are planned as part of this project in the coming months. These tests are intended to expand the knowledge of the behaviour of SMWs and are partially based on the ACI-SEAOSC field tests performed in 1980 [7], which is an often referenced study for full-scale slender walls.

NUMERICAL MODEL

A finite element 2D model was developed using a macro-modeling approach in OpenSEES. A wall of 30 non-linear beam-column type elements, with a support at the base restraining movement along the x and y global axis, and a support at the top restraining movement along the x global axis. The number of segments was selected after a sensitivity test to ensure that the results were accurate enough for the purposes of this work; a higher number of segments triggered a variation of less than 0.01% in the results. The first step in the analysis was to apply a static compressive load P at the top of the wall at an eccentricity, e, both of which are defined by the user. A uniformly distributed load w was then applied along the height of the wall until a target midspan deflection was achieved. A schematic drawing of the model is shown in Figure 1a. Figure 1b shows the simplified section defined in the software, being b = the total width of the wall, w_{gr} = the sum of width of the grouted cells without considering the webs, t = the thickness of the masonry units, and t_f = the maximum face shell thickness, not considering block taper. A_{s1} and A_{s2} are the steel areas for each reinforcement layer, and d_1 and d_2 are their depth relative to the compressive face, respectively. Note that d_2 is d_1 mirrored with respect to the OOP axis for this study. The webs are not modeled because it is assumed that their contribution to the OOP stiffness is negligible.

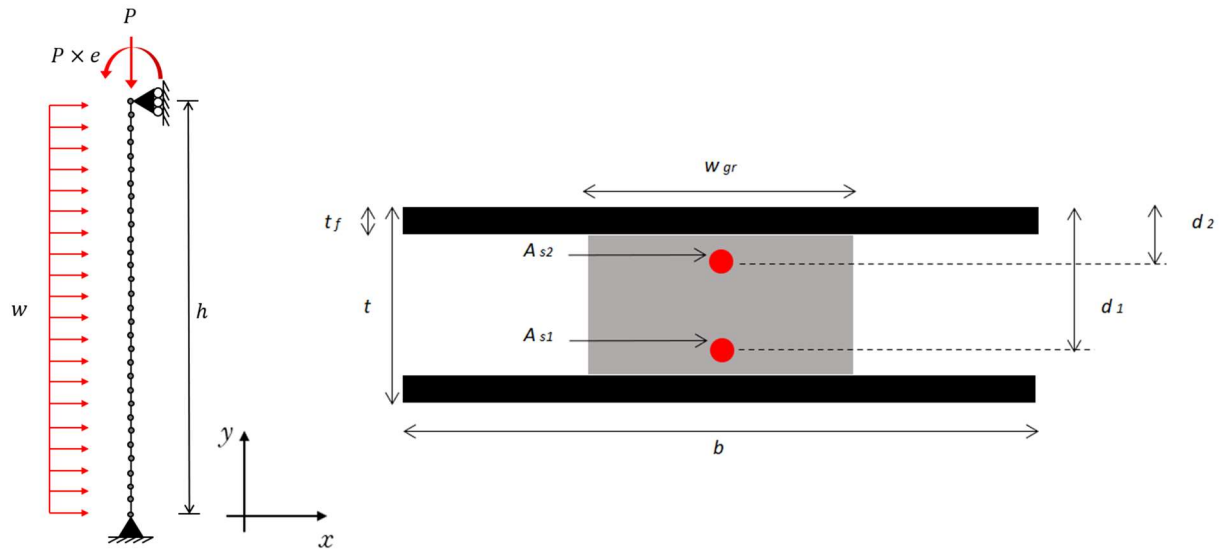

Figure 1: (a) Simplified model of the masonry walls; (b) Simplified cross-section.

Validation

To validate the proposed model, the authors compared model predictions with test results of two completed studies. In the ACI-SEAOSC study [7], nine 1220 mm wide and 7500 mm tall concrete masonry panels were built using different CMU thicknesses. Axial compressive load with an eccentricity of half the thickness of each panel plus 76 mm was applied. A gradually increasing lateral pressure was then induced by an airbag on the wall surface until the engineers determined that the tests were unsafe to continue. Figure 2 shows the lateral load-displacement curves from both the experimental and the numerical results where it is seen that the numerical model predicts

response, including cracking and post-crack displacements reasonably well. Peak loads could not be compared since the physical tests were stopped prior to failure because of safety concerns.

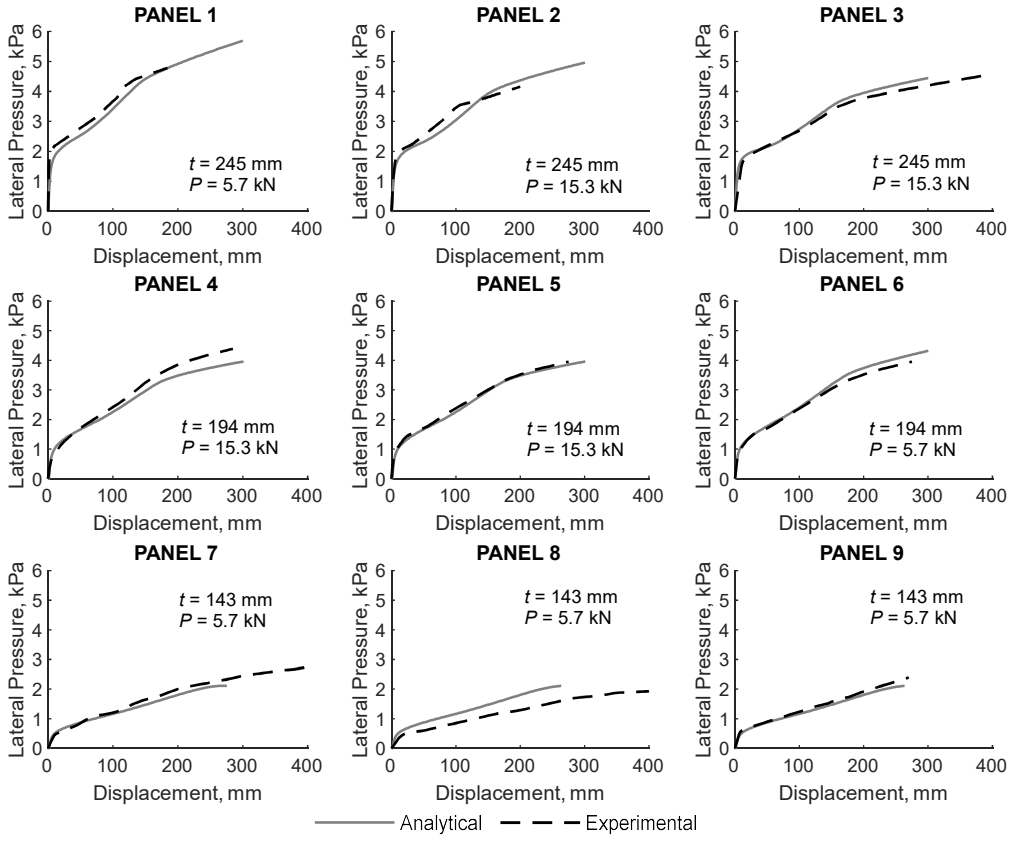

Figure 2: Model vs test midspan displacements of walls under loads (ACI-SEAOSC, 1982).

Liu and Hu [8] applied eccentric compressive load gradually at the top and bottom of twelve 140 × 790 × 2390 mm masonry walls until failure. Figure 3 shows midspan load-displacement curves of four panels, both the analytical and experimental results. Only panels with an eccentricity of zero at the bottom are presented here due to the limitations of the model. Eccentricity values at the top are indicated in each graph. Predictions were close to the measured responses in terms of stiffness as well as failure load. Failure loads were predicted within 5% of the tested values.

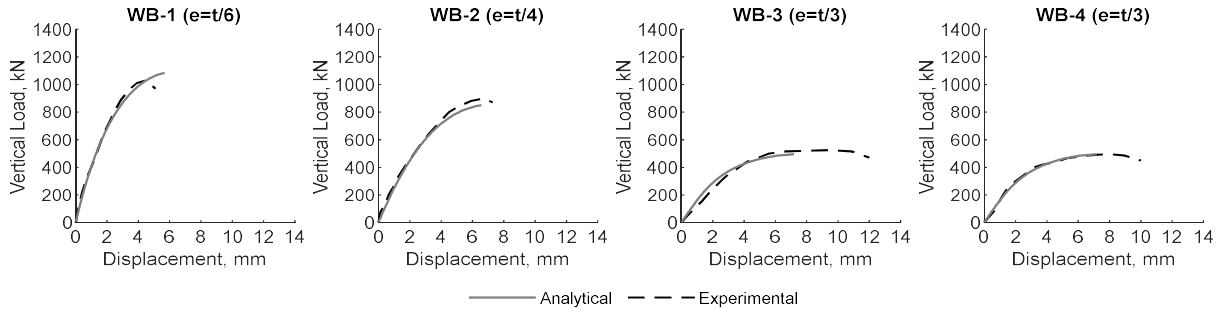

Figure 3: Model vs test midspan displacements of walls under loads (Liu and Hu, 2007).

PARAMETRIC STUDY

A series of static non-linear analyses were performed using the computer models to understand the influence of parameters such as the steel reinforcement ratio and depth, masonry strength and the reinforcement yield stress on SMWs. Panels were defined as 8.75 m tall, with a thickness of 190 mm and a width of 1190 mm. These dimensions result in a slenderness ratio (kh/t) of 46, larger than the limit of 30 given by CSA S304-14. A constant load of 15 kN was selected as an appropriate typical axial load. This compressive load is applied at the top of the wall with an eccentricity of 170 mm, based on the eccentricity values used in the ACI-SEAOSC study [7]. Then, a uniform lateral load is applied until a deflection of 300 mm at midspan was achieved. At this displacement, all walls had passed the point where steel reinforcement yielded. Preliminary drawings of the test setup are displayed in Figure 4.

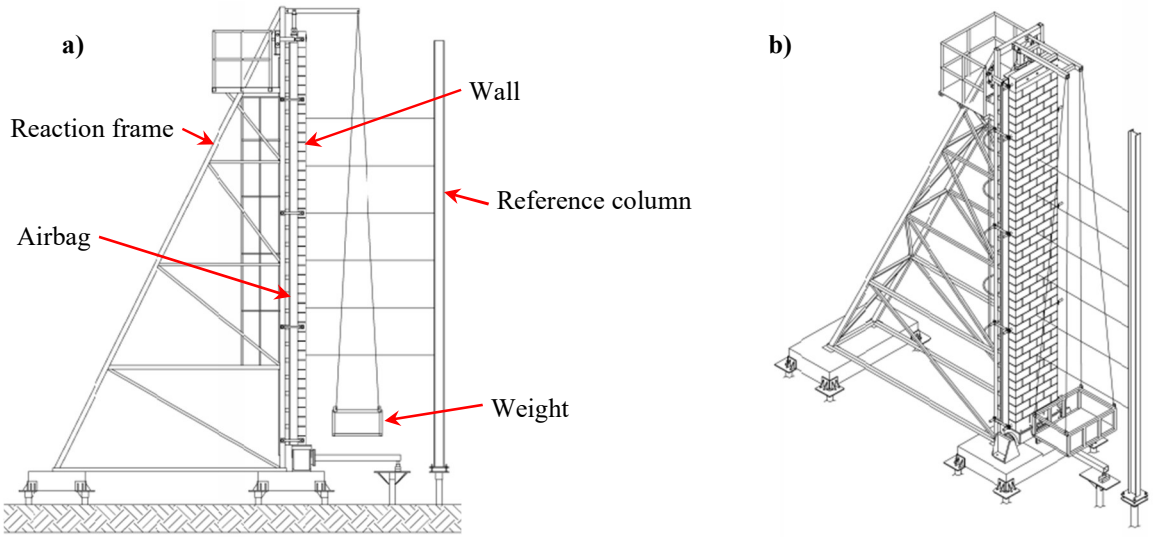

Figure 4: 3D Test setup for testing slender masonry walls: (a) Lateral view; (b) Isometric.

Material properties used in the parametric analyses were based on available experimental data from studies at the University of Alberta [9], conducted in accordance with Canadian standards. These tests results are representative of materials used in Alberta masonry construction. Masonry prisms had a compressive strength (f'_m) of 16.8 MPa, a tensile strength (f_r) of 0.65 MPa, and a maximum-stress strain of 0.002. Steel reinforcement had a yield stress (f_y) of 533 MPa and an elastic modulus (E_s) of 199 GPa. A volumetric weight of 23.6 kN/m^3 was assumed for self-weight calculations of the wall.

Midspan moment-displacement curves from these analyses are presented in Figure 5. Equation (1) was used to calculate total moments at midspan, including both primary and second order moments. Walls were assumed to be single-story with pin-ended conditions as recommended in the Canadian masonry standard.

$$M_{total} = \frac{w \cdot h^2}{8} + \frac{P \cdot e}{2} + (P + P_{sw})\Delta \quad (1)$$

Where w is the uniformly distributed lateral load due to wind obtained by multiplying wind pressure times the wall width, h is the total height of the wall, P is the axial compression load applied to the top support, e is the eccentricity of the axial load, P_{sw} is the axial load due to self weight in the centre of the wall which is half the total self weight, and Δ is the total deflection.

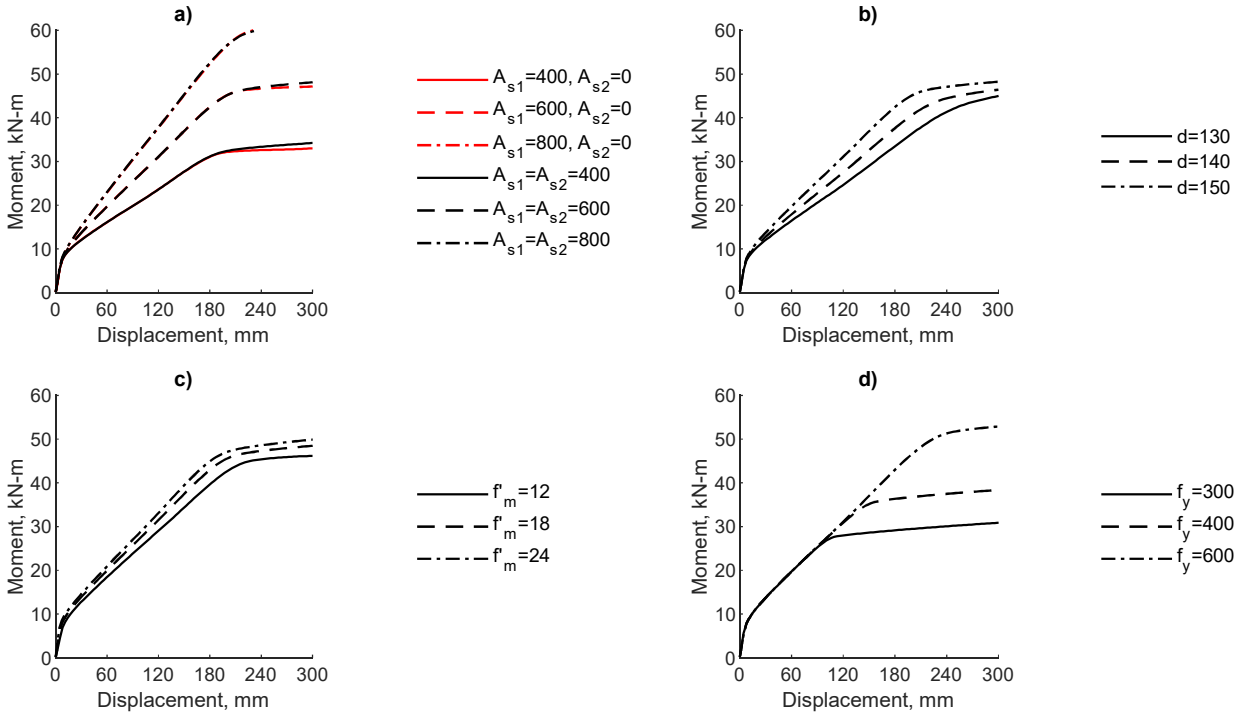

Figure 5: Midspan moment-displacement curves from the parametric study: (a) Changing reinforcement ratio; (b) Changing reinforcement depth; (c) Changing masonry compressive strength; (d) Changing reinforcement yield strength.

The first parameter evaluated was steel ratio (ρ), defined as the total steel area divided by the gross cross-sectional area. All other properties remain fixed. Figure 5a shows responses of walls with different values of ρ. The first three ratios correspond to steel areas of 400, 600 and 800 mm^2 in each layer. The contribution of the compression steel was neglected. The other three, with the same steel area ratios, account for effects that the compression steel may have. The depth of each steel rebar layer was 40 and 150 mm, respectively. Before the cracking moment, at about 7 kNm, there is a negligible difference in the responses of any of the walls. This continues to be true even when other different parameters are varied. After cracking, there is a significant difference in the stiffness of walls with different ρ values, but the effect of the compressive rebar is negligible. According to the model data, this layer of reinforcement was subject to tensile stresses right after cracking occurred. This happens because the out-of-plane neutral axis moves rapidly towards the compression face of the wall. Thus, the formerly compressive steel shifts to be in tension. This suggests that tying rebar to get the benefits of compressive steel will not provide any enhancement for these walls. After reinforcement yields, the moment resistance effectively plateaus for all walls. Results show that increasing steel area greatly improves the response of slender walls.

The second parameter evaluated was the reinforcement depth (d) of both layers. Values of 130, 140 and 150 mm were selected from possible reinforcing arrangements within the wall, using different distances from the rebar edge to the interior face of the masonry face shell. All other parameters remained fixed. In Figure 5b, curves show that even a slight increase of d results in a higher stiffness after cracking. For instance, at 20 kNm there is a displacement of about 90 mm for a d of 130 mm and about 60 mm for a d of 150 mm, a reduction of 50%. It is important to recall that for slender walls the main goal is to achieve a stiffer section to reduce second-order effects; therefore, increasing d seems like an efficient way of doing so. The yielding moment was close to 45 kNm, followed by a plateau for all three cases.

The third parameter evaluated was the masonry strength (f'_m) using three different values that are likely to be found in practice: 12, 18 and 24 MPa. Figure 5c shows very similar curves for the three cases with a small difference in the slope in all stages of the loading. These can be attributed to the change of the elastic modulus of the masonry (E_m) which is a function of f'_m. Since there is not an important enhancement in the response of the walls, there is no reason to increase f'_m.

The fourth parameter evaluated was the yielding stress of the steel rebar (f_y) using values of 300, 400 and 600 MPa. The value of 400 MPa is by far the most common f_y used in construction but it was still interesting to include other possible values in this analysis. The curves in Figure 5d show that changing f_y only causes a higher yielding moment in the wall with the same stiffness before yielding, so there is no motivation to use a higher f_y.

The fifth parameter evaluated was the wall height. Heights of 3250, 6000 and 8750 mm were defined, resulting in slenderness ratios (kh/t) of 17, 32 and 46, respectively. This comparison (Figure 6) was made to visualize how sensitive these walls are to a change in d from 140 to 150 mm. For the 3750 mm wall, taking 20 kNm as reference, the displacement reduction is about 9%. For the 6000 mm wall the reduction is about 18%, and for the 8750 mm wall it is about 28%. These curves serve as an indication that slender walls can benefit from these small changes.

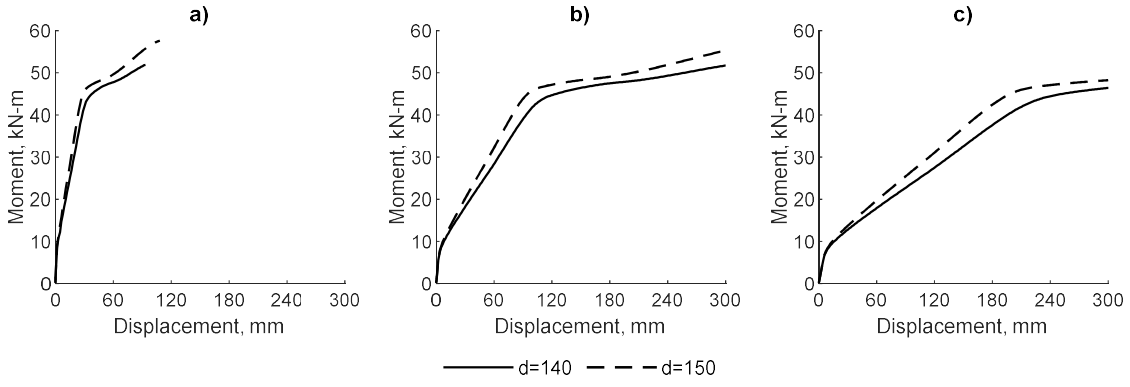

Figure 6: Midspan moment-displacement curves changing the height of the walls: (a) 3750 mm height; (b) 6000 mm height; (c) 8750 mm height.

NEW REINFORCEMENT ARRANGEMENT

From the previous analyses, an arrangement with as much steel area per cell and with the highest reinforcement depth possible is desirable. Increasing ρ and d results in walls with higher out-of-plane stiffnesses. To take advantage of this arrangement the construction process was considered. One limitation is block thickness. Thicker CMUs lead to a stiffer but heavier and more expensive wall. Designing a custom concrete block was an option, but benefits are not sufficient to justify manufacturing costs. Thus, it was decided to work with 20 cm standard units. A second limitation is the hollow cell dimensions and whether cells are grouted or not. Slender walls are sensitive to a change in self-weight, so it was desirable to have the fewest grouted cells that design allows.

The proposal consists of two layers of steel with rebar touching the face shell of the concrete block. This challenges CSA-A371-14 [10] clause 8.2.5.7.1 where the requirement is to have a clear distance of 13 mm between the bar and any masonry surface for coarse grout. By doing this, the reinforcement depth is maximised at the expense of a possible reduction of the bond between the bar and grout. Physical tests will help evaluate if this is a significant effect. The amount of steel in a wall must comply with the minimum area of $0.00125A_g$, where A_g is the gross cross-sectional area, and a maximum of 2% of A_g, according to clauses 10.15.1 and 10.15.2 of CSA-S304-14. Also, the area of vertical reinforcement shall not exceed 6% of the grout space area, as recommended by American standards [11]. Care should be taken with positioning rebar. As discussed before, slender walls are susceptible even a few millimetres change in d. During construction, measures (e.g. stirrups/ties, wire positions) must be used to prevent rebar from shifting from the desired position along the wall height. Confinement benefits of tight tie spacing are negligible for SMWs with low axial loads, and ties may prevent the vertical reinforcement from reaching the edge of the grouted cell. For this, steel wire positioners may be a better choice knowing that a good supervision is needed during construction. Additionally, a proper technique in the application of mortar and the setting of the CMUs is important to minimize mortar fins.

Four 190 × 1190 × 8750 mm PG walls (Figure 7) were defined in the model using the same materials and load conditions as described before. Section 1 represents a typical masonry wall having the rebar positioned at the centre. Section 2 has two layers of reinforcement and the position of the rebar complies with the recommended 13 mm cover from any masonry surface as specified in CSA 304.14. Sections 3 and 4 have two layers of rebar touching the face shell. The difference is that in Section 4, the face shell thickness is slightly reduced from 32 to 28 to gain 4 mm of d. Reducing further this thickness may compromise the loadbearing capacity of the masonry.

Using these four sections, three different steel areas were tested in the model. First, a total steel area of 1600 mm^2 was selected to be within the practical limit of 6% in each cell as specified in the standards, meaning up to 854 mm^2 per cell for 190 mm blocks. This exceeds the maximum steel area recommended by clause 10.7.4.6.5 due to ductility requirements. A second value of 800 mm^2 was selected to comply with the maximum steel area for ductility. A third value of 400 mm^2 is selected to represent a more lightly reinforced wall.

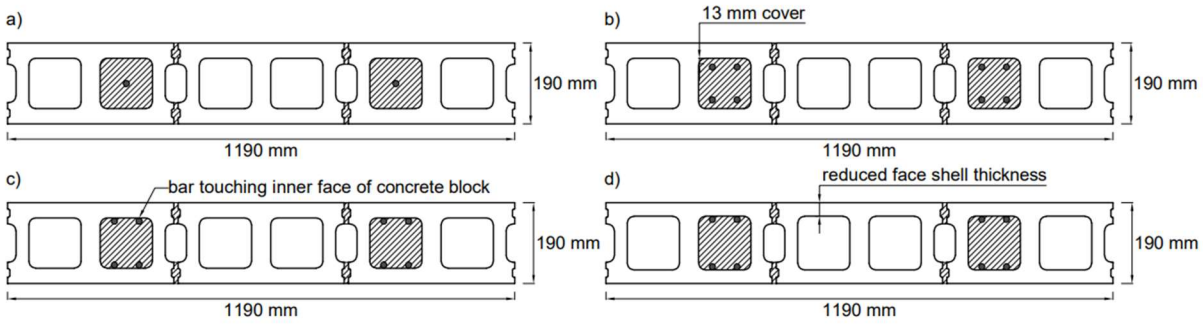

Figure 7: Schematic drawings of cross-sections of the analyzed walls: (a) Section 1, rebar at the centre; (b) Section 2, two layers of reinforcement with 13 mm inner cover; (c) Section 3, two layers with no inner cover; (d) Section 4, CMU with reduced face shell thickness.

RESULTS

Midspan moment-displacement curves for all the walls are shown in Figure 8. In all configurations, no visible change in stiffness is seen before cracking, at about 7 kNm. This portion of the curve is mostly affected by masonry properties since little to no tension is present in the section. For the three groups of walls, sections with a greater reinforcement depth had higher stiffness after cracking, as expected. For all reinforcement ratios, Wall 3 shows a much larger stiffness than Wall 1. For example, taking a reference moment of 15 kNm, displacements are reduced by 35% to 50%. Interestingly Wall 3 is much stiffer than Wall 2 even when the depth increase is only about 13 mm, with displacement reductions of up to 28%. In all cases, Wall 4 response seems close to that of Wall 3, with no significant improvements in either strength or stiffness. It can be assumed that manufacturing a new unit with a reduced thickness is not a feasible way to improve the resistance of these slender walls. Wall 3 has the most promise for evaluation using physical testing.

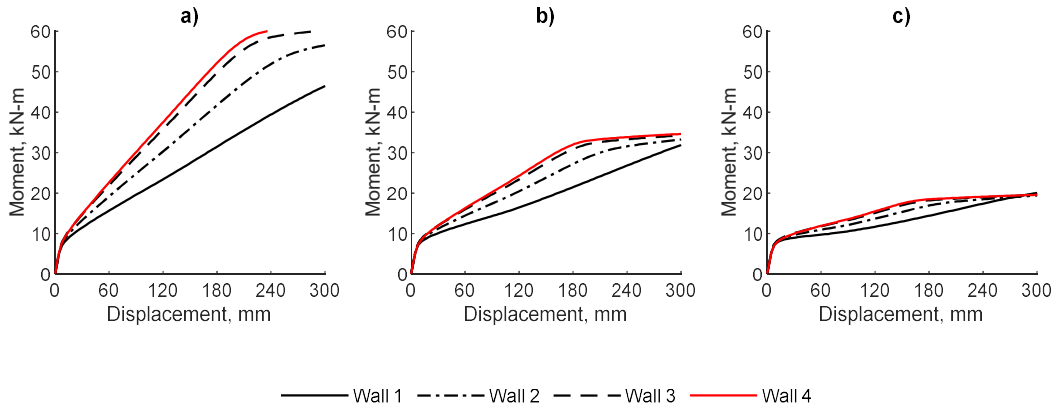

Figure 8: Midspan total moment-displacement curves for 190 × 1190 × 8750 mm walls: (a) A_s = 1600 mm^2; (b) A_s = 800 mm^2; (c) A_s = 400 mm^2.

Differences between wall responses are more drastic in the group with the highest ρ. This group contains an amount of steel that does not comply with the ductility requirement in S304-14. However, it is seen in these curves that yielding occurs after large deflections, immediately

followed by an unstable behaviour. It can be assumed that ductility is not a concern for these slender walls, unlike stability. The third group seems too lightly reinforced for the conditions of the test, since it is evident that after cracking all four sections take large deformations before any noticeable increase in load resistance takes place. Figure 9 shows the same results but with flexural effects decomposed into primary moments and second-order moments at midspan. Because of the slenderness of this walls, second-order effects quickly become important and cause the wall to be unstable at, or even before, the steel has yielded, particularly for the 400 mm^2 walls. These results suggest that the ductility provision should be revised, as it seems to be over-conservative and is preventing designers from using configurations with more steel in the grouted cells.

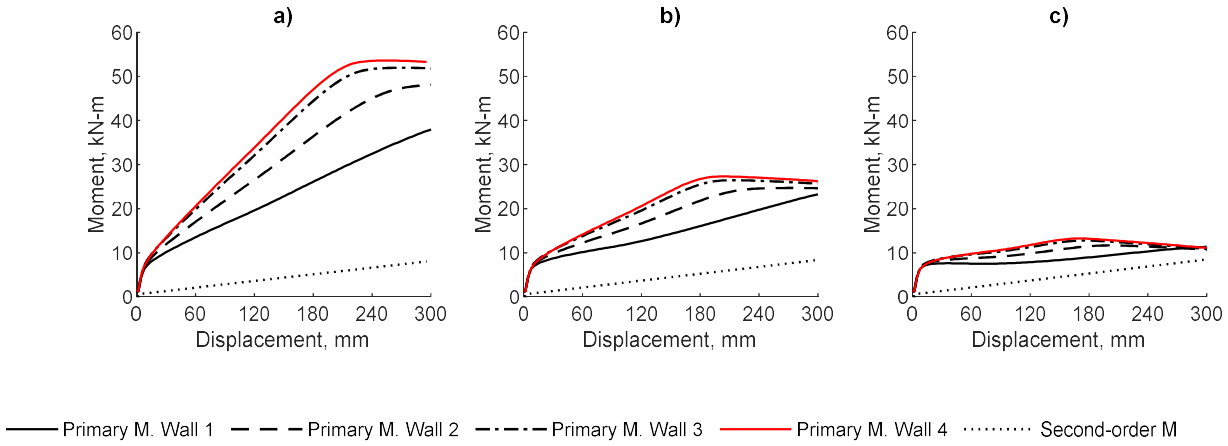

Figure 9: Primary and secondary moments at midspan against displacement for 190 × 1190 × 8750 mm walls: (a) A_s = 1600 mm^2; (b) A_s = 800 mm^2; (c) A_s = 400 mm^2.

CONCLUSIONS

The proposed numerical model proved to be sufficiently accurate for use with typical SMWs subject to low axial loads, and can provide a good understanding of their response under a variety of conditions. Due to the macro-modeling approach, it does not predict any local effects like the crushing of the masonry near the supports, or reduced bonding of the reinforcement.

Wall 3 presents a section where the steel rebar is touching the internal face of the CMU in an effort to increase the moment arm and reduce second-order effects. Physical tests will help to determine the feasibility of this solution, and address the failure mode of these walls.

A more in-depth study must be conducted on the ductility requirements for SMW, found in the CSA-S304-14. Results of this study suggest that slender walls may encounter instability at or before the yielding of the reinforcement, meaning that ductility was of no use. Future studies may explore the failure modes of a wider range SMWs.

ACKNOWLEDGEMENTS

The authors wish to graciously acknowledge the generous contributions and donations from CONACyT, the Masonry Contractors Association of Alberta (MCAA), the Canadian Masonry Design Centre (CMDC) and the Alberta Masonry Council (AMC).

REFERENCES

[1] McKenna, F., Scott, M. H., and Fenves, G. L. (2010). "Nonlinear finite-element analysis software architecture using object composition", *Journal of Computing in Civil Engineering*, 24(1):95-107.

[2] Canadian Standards Association. *S304-14 Design of Masonry Structures*. Mississauga, ON, Canada.

[3] De Lorenzis, L. and Teng, J.G. (2007). "Near-Surface Mounted FRP Reinforcement: An Emerging Technique for Strengthening Structures", *Composites Part B: Engineering*, 32(2), 119-143.

[4] Parvin, A. and Shah, T.S. (2016). "Fiber Reinforced Polymer Strengthening of Structures by NearSurface Mounting Method", *Polymers*, 8(298).

[5] Sparling, A., Palermo, D., and Hashemian, F. (2018). "Out-Of-Plane Flexural Response of Hollow Masonry Walls with Near-Surface Mounted Reinforcement", *10th International Masonry Conference*, Milan, Italy.

[6] Entz, J. (2019). "Development of Innovative in-Line Stiffening Element for Out-of-Plane Masonry Walls", Master's thesis, University of Alberta. Edmonton, AB, Canada.

[7] American Concrete Institute, and Structural Engineers Association of South California (1980). "Report of the task committee on slender walls", Los Angeles, CA, United States.

[8] Liu, Y. and Hu, K. (2007). "Experimental study of reinforced masonry walls subjected to combined axial load and out-of-plane bending", *Can. J. Civ. Eng.*, 34: 1486-1494.

[9] Pettit, C.E.J. (2020). "Effect of Rotational Base Stiffness on the Behaviour of Loadbearing Masonry Walls", Master's thesis, University of Alberta. Edmonton, AB, Canada.

[10] Canadian Standards Association. *A371-14 Masonry construction for buildings*. Toronto, ON, Canada.

[11] Masonry Standards Joint Committee (2002). *Specification for Masonry Structures*, ACI 530.1-02/ ASCE 6-02/TMS 602-02.